This article was downloaded by:
On: *14 January 2011*
Access details: *Access Details: Free Access*
Publisher *Taylor & Francis*
Informa Ltd Registered in England and Wales Registered Number: 1072954 Registered office: Mortimer House, 37-41 Mortimer Street, London W1T 3JH, UK

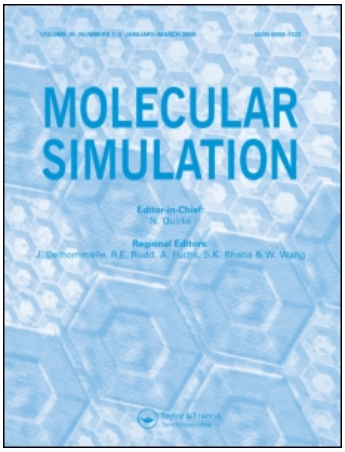

Molecular Simulation
Publication details, including instructions for authors and subscription information:
http://www.informaworld.com/smpp/title~content=t713644482

Perturbed Molecular Dynamics for Calculating Thermal Conductivity of Zirconia

M. Yoshiya[a]; A. Harada[b]; M. Takeuchi[c]; K. Matsunaga[d]; H. Matsubara[a]
[a] Japan Fine Ceramics Center, Nagoya, Japan [b] Fujitsu Kyushu System Engineering Limited, Fukuoka, Japan [c] Fujitsu Limited, Chiba, Japan [d] Institute of Engineering Innovation, The University of Tokyo, Tokyo, Japan

To cite this Article Yoshiya, M. , Harada, A. , Takeuchi, M. , Matsunaga, K. and Matsubara, H.(2004) 'Perturbed Molecular Dynamics for Calculating Thermal Conductivity of Zirconia', Molecular Simulation, 30: 13, 953 — 961
To link to this Article: DOI: 10.1080/08927020410001709389
URL: http://dx.doi.org/10.1080/08927020410001709389

PLEASE SCROLL DOWN FOR ARTICLE

Full terms and conditions of use: http://www.informaworld.com/terms-and-conditions-of-access.pdf

This article may be used for research, teaching and private study purposes. Any substantial or systematic reproduction, re-distribution, re-selling, loan or sub-licensing, systematic supply or distribution in any form to anyone is expressly forbidden.

The publisher does not give any warranty express or implied or make any representation that the contents will be complete or accurate or up to date. The accuracy of any instructions, formulae and drug doses should be independently verified with primary sources. The publisher shall not be liable for any loss, actions, claims, proceedings, demand or costs or damages whatsoever or howsoever caused arising directly or indirectly in connection with or arising out of the use of this material.

Molecular Simulation, Vol. 30 (13–15), 15 November–30 December 2004, pp. 953–961

Taylor & Francis
Taylor & Francis Group

Perturbed Molecular Dynamics for Calculating Thermal Conductivity of Zirconia

M. YOSHIYA[a,*], A. HARADA[b], M. TAKEUCHI[c], K. MATSUNAGA[d] and H. MATSUBARA[a]

[a]*Japan Fine Ceramics Center, 2-4-1 Mutsuno, Atsuta-ku, Nagoya 456-8587, Japan;* [b]*Fujitsu Kyushu System Engineering Limited, Momochihama 2-2-1, Sawara-ku, Fukuoka 814-8589, Japan;* [c]*Fujitsu Limited, Nakase 1-9-3, Mihama-ku, Chiba 261-8588, Japan;* [d]*Institute of Engineering Innovation, The University of Tokyo, 2-11-16, Yayoi, Bunkyo-ku, Tokyo 113-8656, Japan*

(Received 2 February 2004; In final form 3 March 2004)

Downloaded At: 18:28 14 January 2011

A perturbation method is modified to calculate the thermal conductivity of ionic crystals by molecular dynamics simulation. The energy flux and perturbation tensor are formulated so as to contain only phase space variables and a single convergence parameter. The characteristics of the perturbation method are studied using ZrO_2 as a model ionic crystal. The energy flux due to the perturbation is found to exhibit long time-scale oscillations due to the inclusion of long-range Coulombic interactions. In the linear response regime, the calculated thermal conductivity is independent of the external force field parameter, which is the only arbitrary parameter in the method. However, it is found that the external force field parameter plays an important role in minimizing thermal noise in the energy flux. An exponential relationship between thermal conductivity and the maximum external force field parameter is found, by which one can select an external force field parameter suitable for performing thermal conductivity calculations on different ionic materials without needing to carry out numerous preliminary simulations.

Keywords: Molecular dynamics; Thermal conductivity; Zirconia; Perturbation; Non-equilibrium

INTRODUCTION

The reliable calculation of the thermal conductivity of solids is an increasingly important issue from the point of view of materials design. Thermal barrier coatings (TBCs), heat sinks, thermal insulators, IC packaging all rely on control of their thermal conduction properties for their successful application. Furthermore, as nanotechnology proceeds to make smaller and smaller components, the rate of heat dissipation from their small surface areas and volumes becomes critical to their lifetime and performance, so that methods for calculating and predicting thermal conductivities on the atomic level are being eagerly sought.

While thermal conductivity of perfect crystals and materials with single phonon scattering mechanisms are understood well in terms of analytic theories [1,2], the thermal conductivities of real materials are more complex and often deviate from the theoretical values due to impurities and defects that further complicate phonon scattering processes. Such complications are an impediment to the further understanding of heat conduction in solids.

Computer simulations have proven to be effective tools which provide deeper understanding of heat conduction phenomena. In particular, molecular dynamics (MD) based simulations provide quantitative estimates of thermal conductivity via calculations of the phase space trajectory. Although MD simulation is not a replacement for theories, it allows phonon scattering to be quantitatively analyzed by selective introduction of one or more well-characterized phonon scattering sites or mechanisms into a simulation. Recent improvements in computer hardware enable the simulation of complex systems approximating those of real materials, for example, by combining a microscopic method such as MD with a macroscopic method such as finite element analysis.

Calculations of thermal conductivity by MD can be done using one of three methods: (a) the direct method [3–7], (b) the equilibrium method [8–13] and (c) the perturbation method [14–21]. The direct method, which is often referred to as non-equilibrium

*Corresponding author. E-mail: yoshiya@jfcc.or.jp

ISSN 0892-7022 print/ISSN 1029-0435 online © 2004 Taylor & Francis Ltd
DOI: 10.1080/08927020410001709389

Downloaded At: 18:28 14 January 2011

MD (NEMD), imitates experiments: a heat reservoir and a heat sink are attached to a simulation cell and, by the continuous addition and removal at the heat reservoir and heat sink, respectively, a temperature gradient is generated in the cell. By measuring the heat added or removed from the system, or alternatively calculating the microscopic energy flux in the cell, the thermal conductivity is calculated from Fourier's law. This method has the longest history and provides an intuitive description of the heat conduction. However, there are drawbacks in this method. To decrease the artificial effect of the heat reservoir and heat sink, a large cell is required, which makes the simulation computationally expensive. A large temperature gradient that is many orders of magnitude greater than that used in the experiment is needed to reduce the effect of "noise" in the temperature gradient that would otherwise lead to uncertainties in measuring the temperature of the system. In addition, the simulation is never free from artificial phonon scattering at the heat reservoir and heat sink, by which effect the calculated thermal conductivity is underestimated.

In the equilibrium method, thermal conductivity is calculated using the Green–Kubo formula of the fluctuation dissipation theorem [22–24], which provides a connection between heat dissipation as an irreversible process and thermal fluctuations under equilibrium condition. By the use of three dimensional periodic boundary conditions, this method allows thermal conductivity to be calculated without any artificial effects (though there is a cell size dependence). To calculate thermal conductivity in the equilibrium method, the integral of the energy flux autocorrelation function needs to be converged. However, as is generally known, the integral of a Coulombic system exhibits long time-scale oscillations due to the long-range nature of Coulombic interactions, especially in the case of ionic crystals. In addition, thermal noise in the energy flux is included in the integral, which makes convergence quite slow. Consequently, simulations need to be carried out for nano-second, rather than pico-second, time-scales [25].

The perturbation method, also referred to as NEMD, was originally proposed by Ciccotti *et al.* [14] and developed independently by Evans [15] and Gillan and Dixon [17] for simulating Lennard–Jones fluids. In this method, the system is subjected to a perturbation at every time step, which causes heat to flow. (Ciccotti *et al.* prefers a single perturbation to perform subtraction of energy fluxes between perturbed and unperturbed system, which greatly cancels thermal noise for a short time period.) Although it makes use of the Green–Kubo formula, instead of integrating the autocorrelation function of the energy flux, only an average of the energy flux over time is needed to calculate the thermal conductivity. Application of the perturbation to the system greatly reduces the problem due to thermal noise as will be demonstrated. Anisotropy in the thermal conductivity can also be studied by this method. Since the change in temperature between the steady state and equilibrium values is negligibly small [17], the temperature dependence of thermal conductivity can be easily analyzed using this method.

In this study, we have modified the perturbation method to handle Coulombic systems so as to calculate the thermal conductivity of ionic crystals such as ZrO_2 and Y_2O_3-doped ZrO_2, the most commonly used material for TBCs because of its low thermal conductivity. The energy flux and perturbation tensor have been formulated for an ionic system. To ensure reliable thermal conductivity values, the effect of parameters used in the perturbation method have been studied. The structure of the rest of the paper is as follows. In the second section, the theoretical background and the newly formulated perturbation tensor are presented, followed by computational details in the third section. In the fourth section, results obtained for undoped and Y_2O_3-doped ZrO_2 by the perturbation method are reported and the influences of various computational parameters are investigated. Conclusions are given in the fifth section.

THEORY

When a system is subject to a perturbation, the equations of motion for atom i can be written as

$$\dot{\mathbf{r}}_i = \frac{\mathbf{p}_i}{m_i} + \overleftrightarrow{\mathbf{C}}_i \cdot \mathbf{F}_{\text{ext}} \tag{1}$$

$$\dot{\mathbf{p}}_i = \mathbf{F}_i + \overleftrightarrow{\mathbf{D}}_i \cdot \mathbf{F}_{\text{ext}} \tag{2}$$

where $\mathbf{r}_i$ and $\mathbf{p}_i$ are the position and momentum vectors of i, respectively, and $\mathbf{F}_i$ is the force exerted on i. $\overleftrightarrow{\mathbf{C}}_i$ and $\overleftrightarrow{\mathbf{D}}_i$ are the perturbation tensors and $\mathbf{F}_{\text{ext}}$ is the magnitude of the perturbation. These second rank tensors are chosen so that the response of the system to the perturbation corresponds to the properties desired. In this study,

$$\overleftrightarrow{\mathbf{C}}_i = \overleftrightarrow{\mathbf{0}} \tag{3}$$

For perturbations that are small enough for linear response theory [22] to be applicable, the Hamiltonian of a system, H_0, changes at a rate

$$\dot{H}_0 = \sum_i \left(\frac{\partial H_0}{\partial \mathbf{p}_i} \frac{\partial \mathbf{p}_i}{\partial t} + \frac{\partial H_0}{\partial \mathbb{r}_i} \frac{\partial \mathbb{r}_i}{\partial t} \right). \tag{4}$$

Substituting Eqs. (1)–(3) in (4) yields

$$\dot{H}_0 = \sum_i \left(\frac{\mathbf{p}_i \cdot (\overleftrightarrow{\mathbf{D}}_i \cdot \mathbf{F}_{\text{ext}})}{m_i} \right) \tag{5}$$

Downloaded At: 18:28 14 January 2011

which is the response of the system to the perturbation. The ensemble average at time t of energy flux vector, $\mathbf{J}$, in the linear response regime is given by

$$\langle \mathbf{J} \rangle_t = \langle \mathbf{J} \rangle_c + \frac{1}{k_B T} \int_0^t \langle \mathbf{J}(\tau) \dot{H}_0(0) \rangle \, d\tau \tag{6}$$

where $\mathbf{J}$ is an instantaneous microscopic energy flux vector, $\langle \mathbf{J} \rangle_o$ is the equilibrium average of the energy flux, which tends to 0 as time tends to infinity, k_B is Boltzmann's constant, and T is the temperature of the system. Time is measured from when the perturbation is introduced to the system. On the other hand, according to the Green–Kubo formula [22,23], thermal conductivity, κ, can be calculated as,

$$\kappa = \frac{V}{k_B T^2} \int_0^\infty \langle J_x(\tau) J_x(0) \rangle \, d\tau \tag{7}$$

where V is the volume of the system and J_x is the component of $\mathbf{J}$ along the x direction. The essence of the perturbation method is that, if we choose perturbation tensor, $\overleftrightarrow{\mathbf{D}}_i$, such that the linear response of the system corresponds to an element of the energy flux, the thermal conductivity can be calculated without integrating the energy flux as in Eq. (7) [14, 15, 17]. This requires

$$\dot{H}_0 = \sum_i \left(\frac{\mathbf{p}_i \cdot (\overleftrightarrow{\mathbf{D}}_i \cdot \mathbf{F}_{ext})}{m_i} \right) = \mathbf{J} \cdot \mathbf{F}_{ext}. \tag{8}$$

Therefore,

$$\mathbf{J} = \sum_i \left(\frac{\mathbf{p}_i \cdot \overleftrightarrow{\mathbf{D}}_i}{m_i} \right). \tag{9}$$

Usually, the perturbation is applied in one direction only, i.e.

$$\mathbf{F}_{ext} = \begin{pmatrix} F_{ext} \\ 0 \\ 0 \end{pmatrix}. \tag{10}$$

Substituting Eqs. (9) and (10) in (6) yields

$$\langle J_x \rangle_t = \frac{F_{ext}}{k_B T} \int_0^t \langle J_x(\tau) J_x(0) \rangle \, d\tau. \tag{11}$$

By comparing Eqs. (7) and (11), we obtain

$$\kappa = \frac{V}{\mathbf{F}_{ext} T} \lim_{t \to \infty} \langle J_x \rangle_t, \tag{12}$$

i.e. the thermal conductivity can be calculated by simply averaging the instantaneous energy flux resulting from the perturbation instead of integrating it as in Eq. (7).

A microscopic form of the energy flux vector is given by Irving and Kirkwood [26] as

$$\mathbf{J} = \frac{1}{2V} \sum_i \left[\left\{ m_i \left| \frac{\mathbf{p}_i}{m_i} \right|^2 + \sum_j \phi_{ij} \overleftrightarrow{\mathbf{I}} \right\} \frac{\mathbf{p}_i}{m_i} - \sum_j \left(\mathbf{F}_{ij} \cdot \frac{\mathbf{p}_i}{m_i} \right) \mathbf{r}_{ij} \right] \tag{13}$$

where ϕ_{ij} is the interatomic potential energy as a function of interatomic distance including the Coulomb energy, $\overleftrightarrow{\mathbf{I}}$ is a unit tensor, $\mathbf{F}_{ij}$ is the force on i exerted by j and $\mathbf{r}_{ij} \equiv \mathbf{r}_j - \mathbf{r}_i$. This equation assumes the center of mass of the system remains at the same place, which is justified when the initial velocity of the system is zero and the total momentum in the equations of motion is preserved. The last term in Eq. (13) is the most troublesome for Coulombic systems. Energy and force are calculated as the sums of a short range term and the Coulombic term. The latter is usually calculated by the well-known Ewald method [27–29], which divides the calculation of the energy and force into a real space term, a reciprocal space term, and a self-interaction term which vanishes in the force calculation. The long-range Coulombic force of atom i, $\mathbf{F}_i$, can be written as

$$\mathbf{F}_i = \mathbf{F}_i^{real} + \mathbf{F}_i^{reciprocal} \tag{14}$$

$$\mathbf{F}_i^{real} = \sum_j \mathbf{f}_{ij}^{real} \tag{15}$$

$$\mathbf{F}_i^{reciprocal} = \sum_j \sum_{\mathbf{k}} \mathbf{f}_{ij}^{reciprocal}(\mathbf{k}) \tag{16}$$

where superscripts real and reciprocal in Eq. (14) denote real space sum and reciprocal sum, respectively, and $\mathbf{k}$ is the reciprocal lattice vector. The real space term involves a sum over j, and thus simply taking a component $\mathbf{f}_{ij}^{real}$ out of the force sum gives the term for $\mathbf{F}_{ij}$. The reciprocal term is also given by a sum over j in addition to a sum over the wave number vector. However, in the case of the reciprocal space term, taking a component $\sum_{\mathbf{k}} \mathbf{f}_{ij}^{reciprocal}(\mathbf{k})$ out of the force sum does not give the force exerted by j on i. It actually gives the sum of forces exerted by j and its periodic images on i due to the nature of reciprocal space. The product of $\mathbf{F}_{ij}$ and $\mathbf{p}_i/m_i$ is multiplied by $\mathbf{r}_{ij}$ in Eq. (13). Thus, if $\mathbf{F}_{ij}$ is calculated by the conventional Ewald method, $\mathbf{J}$ is overestimated. Therefore, although this error becomes smaller as the cell size increases, the conventional Ewald method cannot be used in the calculation of the energy flux.

By solving the continuity equation in reciprocal space, Bernu and Vieillefosse formulated the energy flux vector for a one-component plasma [30]. It can readily be modified for ionic systems as [11,12,31].

$$J_x = \frac{1}{2V} \sum_i \left\{ m_i \left| \frac{\mathbf{p}_i}{m_i} \right|^2 \frac{p_{ix}}{m_i} + \sum_{j \neq i} \left(\phi^{SR} \frac{p_{ix}}{m_i} - \frac{d\phi^{SR}}{d|\mathbf{r}_{ij}|} \frac{r_{ijx}}{|\mathbf{r}_{ij}|} \mathbf{r}_{ij} \right) \right\} + J_x^{Coulomb} \tag{17}$$

$$J_x^{\text{Coulomb}} = \frac{1}{V}\sum_{\mathbf{k}\neq 0}\frac{4\pi}{|\mathbf{k}|^2}\exp\left(-\frac{|\mathbf{k}|^2}{4\alpha^2}\right) \times\sum_i\left\{\left(1-\frac{|\mathbf{k}|^2}{4\alpha^2}\right)\frac{p_{ix}}{m_i}-\left(1+\frac{|\mathbf{k}|^2}{4\alpha^2}\right)\hat{k}_x\frac{\mathbf{p}_i}{m_i}\cdot\hat{\mathbf{k}}\right\} \times\left\{Z_i\cos(\mathbf{k}\cdot\mathbf{r}_i)\sum_{j\neq i}Z_j\cos(\mathbf{k}\cdot\mathbf{r}_j) +Z_i\sin(\mathbf{k}\cdot\mathbf{r}_i)\sum_{j\neq i}Z_j\sin(\mathbf{k}\cdot\mathbf{r}_j)\right\} +\sum_i\sum_j\frac{Z_iZ_j}{2V}\sum_\lambda\left\{\frac{p_{ix}}{m_i}+\frac{\mathbf{p}_i}{m_i}\cdot\frac{\mathbf{r}_{ij}+\boldsymbol{\lambda}}{|\mathbf{r}_{ij}+\boldsymbol{\lambda}|}\left(\frac{r_{ijx}+\lambda_x}{|\mathbf{r}_{ij}+\boldsymbol{\lambda}|}\right)\right\} \times\left\{\frac{\operatorname{erfc}\left(\alpha|\mathbf{r}_{ij}+\boldsymbol{\lambda}|\right)}{|\mathbf{r}_{ij}+\boldsymbol{\lambda}|}+\frac{2\alpha}{\sqrt{\pi}}\exp\left(-\alpha^2|\mathbf{r}_{ij}+\boldsymbol{\lambda}|^2\right)\right\} -\sum_i\sum_{j\neq i}\frac{Z_iZ_j}{V}\frac{2\pi}{\alpha^2}\frac{p_{ix}}{m_i} \tag{18}$$

where ϕ^{SR} denotes short range potential energy, $\mathbf{k}$ and $\boldsymbol{\lambda}$ are reciprocal and direct lattice vectors, respectively, $\hat{\mathbf{k}}$ is the unit vector in the direction of $\mathbf{k}$ and Z_i is the charge of ion i. Subscript x denotes that it is an x component. The parameter α only determines the speed of convergence, as in the conventional Ewald method, and does not affect the value of the energy flux when chosen properly. Thus, although Eq. (18) appears to be complicated, the energy flux can be readily calculated using phase space variables only as in Eq. (13). The perturbation tensor can be determined from Eqs. (8), (17) and (18) according to

$$\overleftrightarrow{\mathbf{D}}_i^{\text{raw}} = \overleftrightarrow{\mathbf{D}}_i^{\text{Non-Coulomb}} + \overleftrightarrow{\mathbf{D}}_i^{\text{Coulomb}} \tag{19}$$

$$\mathbf{D}_i^{\text{Non-Coulomb}} = \frac{1}{2V}\left(m_i\left|\frac{\mathbf{p}_i}{m_i}\right|^2+\sum_{j\neq i}\phi^{\text{SR}}\right)\overleftrightarrow{\mathbf{I}}-\overleftrightarrow{\mathbf{Q}} \tag{20}$$

$$\overleftrightarrow{\mathbf{D}}_i^{\text{Coulomb}} = \left[\frac{1}{V}\sum_{\mathbf{k}\neq 0}\frac{4\pi}{|\mathbf{k}|^2}\exp\left(-\frac{|\mathbf{k}|^2}{4\alpha^2}\right)\sum_i\left(1-\frac{|\mathbf{k}|^2}{4\alpha^2}\right) \times\left\{Z_i\cos(\mathbf{k}\cdot\mathbf{r}_i)\sum_{j\neq i}Z_j\cos(\mathbf{k}\cdot\mathbf{r}_j) +Z_i\sin(\mathbf{k}\cdot\mathbf{r}_i)\sum_{j\neq i}Z_j\sin(\mathbf{k}\cdot\mathbf{r}_j)\right\} +\sum_j\frac{Z_iZ_j}{2V}\sum_\lambda\left\{\frac{\operatorname{erfc}(\alpha|\mathbf{r}_{ij}+\boldsymbol{\lambda}|)}{|\mathbf{r}_{ij}+\boldsymbol{\lambda}|} +\frac{2\alpha}{\sqrt{\pi}}\exp(-\alpha^2|\mathbf{r}_{ij}+\boldsymbol{\lambda}|^2)\right\}-\sum_{j\neq i}\frac{Z_iZ_j}{2V}\frac{2\pi}{\alpha^2}\right]\overleftrightarrow{\mathbf{I}}-\overleftrightarrow{\mathbf{R}} \tag{21}$$

where elements of $\overleftrightarrow{\mathbf{Q}}$ and $\overleftrightarrow{\mathbf{R}}$ are given by

$$Q_{ab} = \frac{1}{V}\frac{d\phi^{\text{SR}}}{d|\mathbf{r}_{ij}|}\frac{r_{ija}}{|\mathbf{r}_{ij}|}r_{ijb} \tag{22}$$

and

$$R_{ab} = \frac{1}{V}\sum_{\mathbf{k}\neq 0}\frac{4\pi}{|\mathbf{k}|^2}\left(1+\frac{|\mathbf{k}|^2}{4\alpha^2}\right)\hat{k}_a\hat{k}_b\exp\left(-\frac{|\mathbf{k}|^2}{4\alpha^2}\right) \times\left\{Z_i\cos(\mathbf{k}\cdot\mathbf{r}_i)\sum_{j\neq i}Z_j\cos(\mathbf{k}\cdot\mathbf{r}_j)+Z_i\sin(\mathbf{k}\cdot\mathbf{r}_i) \times\sum_{j\neq i}Z_j\sin(\mathbf{k}\cdot\mathbf{r}_j)\right\} -\sum_j\frac{Z_iZ_j}{2V}\sum_\lambda\frac{r_{ija}+\lambda_a}{|\mathbf{r}_{ij}+\boldsymbol{\lambda}|}\frac{r_{ijb}+\lambda_b}{|\mathbf{r}_{ij}+\boldsymbol{\lambda}|} \times\left\{\frac{\operatorname{erfc}(\alpha|\mathbf{r}_{ij}+\lambda|)}{|\mathbf{r}_{ij}+\lambda|}+\frac{2\alpha}{\sqrt{\pi}}\exp(-\alpha^2|\mathbf{r}_{ij}+\boldsymbol{\lambda}|^2)\right\} \tag{23}$$

The total momentum of the system is preserved when

$$\sum_i\overleftrightarrow{\mathbf{D}}_i = \overleftrightarrow{\mathbf{0}} \tag{24}$$

To satisfy this relation, Evans proposed taking the difference between the perturbation tensor and its average in the system [15]. Paolini and Ciccotti extended this idea to taking the average for each species [21], i.e.

$$\overleftrightarrow{\mathbf{D}}_i = \overleftrightarrow{\mathbf{D}}_i^{\text{raw}} - \frac{1}{N_\mu}\sum_{i\subset\mu}\overleftrightarrow{\mathbf{D}}_i^{\text{raw}} \tag{25}$$

where N_μ is the number of species μ. This is the perturbation tensor that needs to be substituted into the equations of motion, Eq. (2). This perturbation tensor satisfies Eq. (24) and, thus, the total momentum of the system is preserved. To prevent the system from being continually heated by the perturbation, a thermostat is needed. We employed the Nosé–Hoover thermostat method [32,33], which preserves the total momentum of the system, so that its inclusion does not violate the condition of Eq. (24).

TECHNICAL DETAILS

A Buckingham type pair-wise potential function was employed to describe short-range interatomic energy and force. The function has the form

$$\phi_{ij}^{SR}(|\mathbf{r}_{ij}|) = A_{ij}\exp\left(-\frac{|\mathbf{r}_{ij}|}{\rho_{ij}}\right)-\frac{B_{ij}}{|\mathbf{r}_{ij}|^6}+\frac{Z_iZ_j}{|\mathbf{r}_{ij}|} \tag{26}$$

where A_{ij}, ρ_{ij} and B_{ij} are parameters for each ion–ion pair. In this study, the parameters reported by

Downloaded At: 18:28 14 January 2011

Schelling and Phillpot [5] were used. The phonon density of states obtained by lattice dynamics using these potential parameters reproduced well experimental results and that obtained by first principles calculation. These parameters were obtained by fitting to the thermal expansion coefficient, ensuring that the anharmonicity in the atomic interaction, which is responsible for the decrease in thermal conductivity at high temperature, was reproduced well. Although the low temperature monoclinic phase of ZrO_2 was not reproduced, the phase transition between the cubic and tetragonal phases was satisfactorily reproduced by these parameters. It was found, however, that the sound velocity in the crystal calculated with these potentials was a little higher than experimental values, which results in an overestimation of the thermal conductivity.

Preliminary results showed that there is a cell size dependence for the thermal conductivity, but the values are almost converged when the cell size is increased to $6 \times 6 \times 6$ unit cells, in other words, 864 Zr^{4+} ions and 1728 O^{2-} ions. For 4 mol% Y_2O_3-doped ZrO_2, Y^{3+} ions and O^{2-} vacancies were randomly substituted for Zr^{4+} and O^{2-}, respectively. No configurational dependence for thermal conductivity was found when substitution sites are chosen randomly.

Simulations using the perturbation method were performed at fixed volumes estimated from independent simulations in NTP ensemble using the Parrinello–Rahman method [34]. The perturbation was applied to the system after thermalizing for 25 ps using a temperature scaling technique and for 25 ps using the Nosé–Hoover thermostat. The external force field parameter, F_{ext}, was deliberately chosen so that the response of the system lies within the linear response regime. The time step was chosen to be 1 fs. All simulations were performed using the Materials Explores code [35] after being modified for carrying out the thermal conductivity calculations.

RESULTS AND DISCUSSION

The energy flux caused by the perturbation inherits the behavior of the Green–Kubo formula. Thus, the energy flux behaves in the same way as the Green–Kubo integration in terms of time evolution. According to the literature [11,12,17], in the case of fluids or molten salts, the autocorrelation function of the energy flux, i.e. integrand of the Green–Kubo formula, quickly diminishes to zero as time τ in Eq. (7) increases. Thus, its integral quickly converges to a value from which the thermal conductivity is calculated. However, the time evolution of the Green–Kubo integral or the energy flux due to the perturbation in ionic crystals is likely to be different since there exists a long-range Coulombic force.

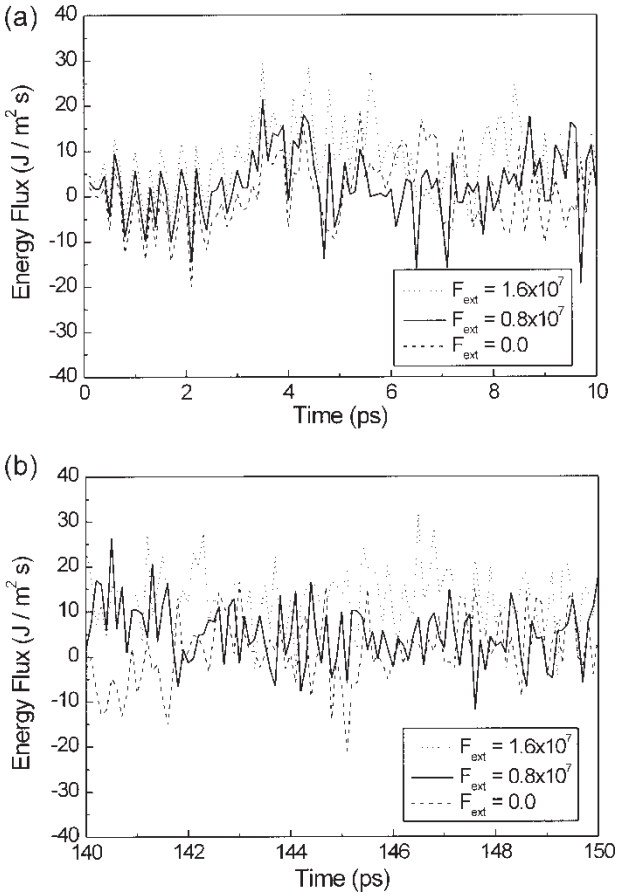

FIGURE 1 Time evolution of energy flux due to perturbation in undoped ZrO_2 at 400 K (a) for the first 10 ps and (b) for the last 10 ps.

Figure 1 shows the time evolution of the energy flux due to the perturbation for the first and last 10 ps out of a 150 ps simulation for perturbations of three different magnitudes. Just after the perturbation is introduced at $t = 0$ in each simulation, the oscillations in the heat fluxes are highly correlated, as shown in Fig. 1(a). This indicates that the perturbations only slightly modify the thermal fluctuation at equilibrium by driving existing modes. After 5 ps, the energy fluxes start to deviate from each other. At the end of 150 ps run, the heat fluxes have become almost independent of each other, although the phase space trajectories for the three cases before the perturbation was applied were exactly the same. This can be attributed to Lyapunov instability [36], which makes the phase space trajectories almost independent of each other. Thus, energy flux averages over long simulations with different external force field parameters, F_{ext}, are almost statistically independent, giving a value of thermal conductivity averaged not only over time but also over ensembles.

As shown in Fig. 1(a), the time evolution of the energy flux appears to be quite different from that found in the literature. It did not increase at

Downloaded At: 18:28 14 January 2011

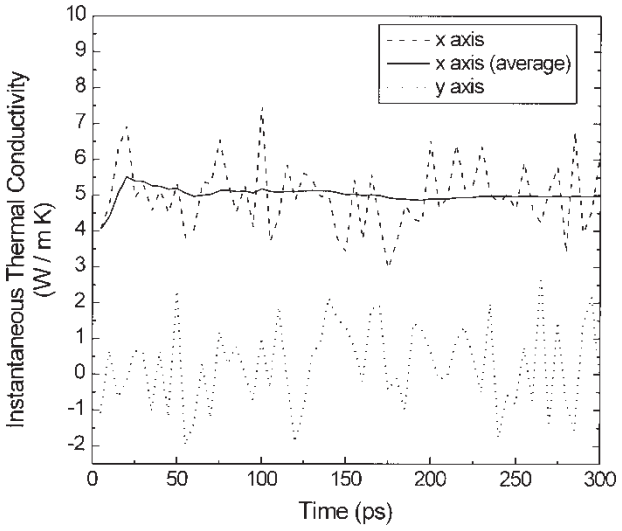

FIGURE 2 Instantaneous thermal conductivity as a function of time for undoped ZrO_2 at 2000 K. Each data point represents a 5 ps average. The x-axis average is shown as a function of the time over which the average was taken.

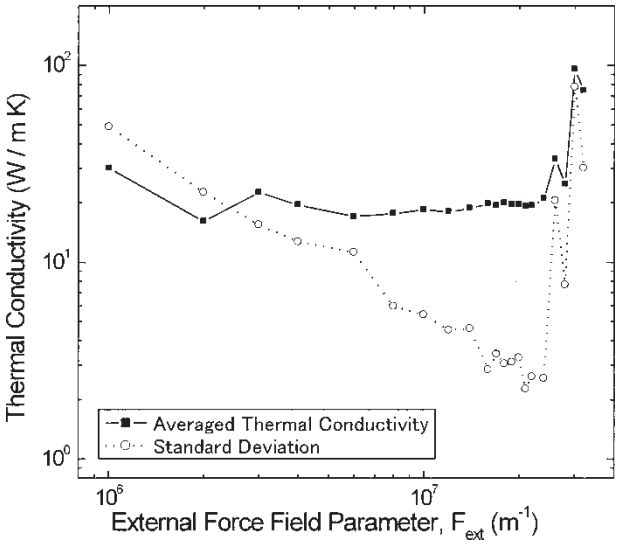

FIGURE 3 Average thermal conductivity as a function of magnitude of the perturbation. Below $2.2 \times 10^7\,\mathrm{m}^{-1}$, the response of the system can be described by the linear response theory.

Downloaded At: 18:28 14 January 2011

the beginning or converge within 10 ps. Instead, it oscillates significantly. After 140 ps, as seen in Fig. 1(b), the energy flux seems to have a non-zero average which depends on the external force field parameter, F_{ext}. Due to its oscillating behavior, it is difficult to judge whether the energy flux has converged or not by only monitoring instantaneous values. Figure 2 shows the variation of the average value of thermal conductivity along the x-axis, i.e. the perturbed energy flux multiplied by $V/F_{ext}T$. Instantaneous values obtained by averaging for 5 ps in the x and y directions are also shown. The perturbations were applied in the x direction only. It can clearly be seen that the x component of the energy flux has a non-zero average while that of the y component is zero. Although instantaneous values oscillate greatly due to thermal fluctuation, it is found that the average value has almost converged at around 150 ps. This demonstrates that the time needed to obtain reliable thermal conductivity values using the perturbation method is longer in the case of ionic crystals than for non-ionic fluids, but much shorter than in the equilibrium method. This is in part due to the simplicity of the averaging step compared to integration, which tends to sum up statistical noise, and is a clear advantage of the perturbation method.

The external force field parameter, F_{ext}, is the only parameter other than phase space variables. Although its contribution to the simulation is cancelled out in Eq. (12), the dependence of thermal conductivity on F_{ext} needs to be investigated to ensure calculated values are reliable. Figure 3 shows thermal conductivity, obtained by averaging instantaneous values for 300 ps, as a function of F_{ext}. The standard deviation estimated using the 5 ps averages of the instantaneous thermal conductivity is also shown. This plot shows that the thermal conductivity is independent of F_{ext} when $F_{ext} \leq 2.2 \times 10^7\,\mathrm{m}^{-1}$. This is the range in which the response of the system to the perturbation can be described by linear response theory [22]. Just above this range, $F_{ext} = 2.4 \times 10^7$, the thermal conductivity is slightly increased and linear response theory become invalid. Further jumps in the thermal conductivity value by factors of magnitude occur as F_{ext} is increased further. Since the perturbation method assumes linear response theory to be valid, thermal conductivity values obtained above this range do not have any physical meaning. The standard deviation exponentially decreases with increasing F_{ext} when $F_{ext} \leq 2.2 \times 10^7\,\mathrm{m}^{-1}$. Above the linear response range, the standard deviation also jumps in conjunction with the apparent thermal conductivity. The standard deviation in the linear response range can be attributed to the thermal fluctuations in the energy flux. The fluctuation is independent of F_{ext}. As shown in Eq. (12), the energy flux is divided by F_{ext} to obtain the thermal conductivity. Hence, the contribution of the thermal fluctuations in the energy flux can be significantly reduced by increasing the magnitude of the perturbation. This is another advantage of the perturbation method over the equilibrium method in which the thermal conductivity value is greatly influenced by thermal fluctuations in the heat flux.

In order to obtain reliable values of thermal conductivity, F_{ext} must be within the linear response range. To minimize the error in the calculated thermal conductivity, F_{ext} needs to be large enough to give a small standard deviation. These two requirements suggest that F_{ext} should be just below the upper limit

Downloaded At: 18:28 14 January 2011

of F_{ext} in the linear response range. However, performing simulations for a number of different F_{ext} values to determine the optimum F_{ext} is time consuming and computationally expensive, making it impractical for routine use.

The maximum F_{ext} for both undoped ZrO_2 and Y_2O_3-doped ZrO_2 for various temperatures are plotted as a function of thermal conductivity in Fig. 4. It should be noted that the maximum F_{ext} in the figure was determined from relatively short time simulations (25 ps), and thus, values might be smaller for longer simulations in which the probability of deviating from linear response regime is larger. Surprisingly, all the data lie on a single exponential line, independent of temperature, despite the fact that phonon transport is strongly altered by addition of Y_2O_3. The relationship can be described by

$$F_{ext}^{max} = 10^M \times \kappa^{-N} \tag{27}$$

where M and N are calculated by fitting to be 8.82 and 1.14, respectively. For force field parameters below this line, linear response theory holds. Considering the fact that the boundary separating the linear response region from the non-linear region is not very abrupt, values of F_{ext} reasonably well below the line instead of on the line are to be preferred.

Because of its simplicity, the relationship between F_{ext} and κ can be used as a guide to selecting F_{ext}. If one roughly knows the value of κ, at least its order of magnitude, an F_{ext} that produces a perturbation within the linear response regime can be easily estimated without repeating numerous simulations using various F_{ext} values. This relationship can be determined in the following way. As shown in Fig. 1, the perturbation modifies the motions of the particles only slightly. Depending on the components of the perturbation tensor **D**, the particles in the simulation cell receive kinetic energy from the perturbation. The added energy dissipates from the particle by interaction with the surrounding particles. Finally, the dissipated energy is absorbed by the heat bath of the thermostat. When the energy received at a time step cannot be removed from the particle by dissipation before more energy is received in the next time step, kinetic energy of the particle increases further. The imbalance between the rate of energy dissipation and the magnitude of the perturbation finally results in exceeding the linear response limit. By definition, the dissipation of the excess energy is related to thermal conductivity. Thus, the maximum external force field parameter for the system to stay within the linear response regime is intimately related to the thermal conductivity of the system.

Finally, the temperature dependence of the thermal conductivity of undoped ZrO_2 and 4 mol% Y_2O_3-doped ZrO_2 are shown in Fig. 5. Each data point was obtained from a single 300 ps simulation, and thus contains a relatively large statistical error. The thermal conductivity of undoped ZrO_2 at 400 K is somewhat higher than that obtained by the direct method using the same potential parameters [5]. This can be ascribed to the absence of artificial phonon scattering at the heat reservoir and heat sink as occurs with the direct method. The temperature dependence of undoped ZrO_2 can be fitted to a smooth curve similar to that predicted by analytical theories [1] and experiment [37]. This is in contrast to the deviation from the smooth curve at 400 and 2000 K calculated using the direct method [5]. This demonstrates the superiority of the perturbation method over a wide range of temperatures. In addition, the significant decrease in thermal conductivity caused by Y_2O_3

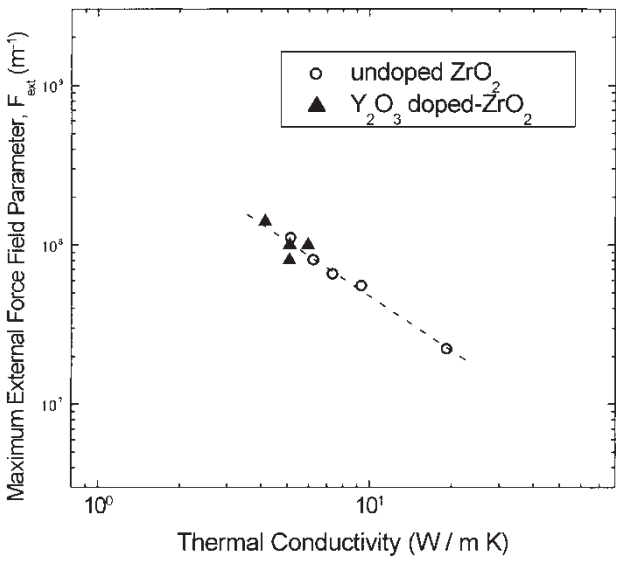

FIGURE 4 Relationship between thermal conductivity and maximum external force field parameter for linear response. Data for both undoped ZrO_2 and Y_2O_3-doped ZrO_2 are shown.

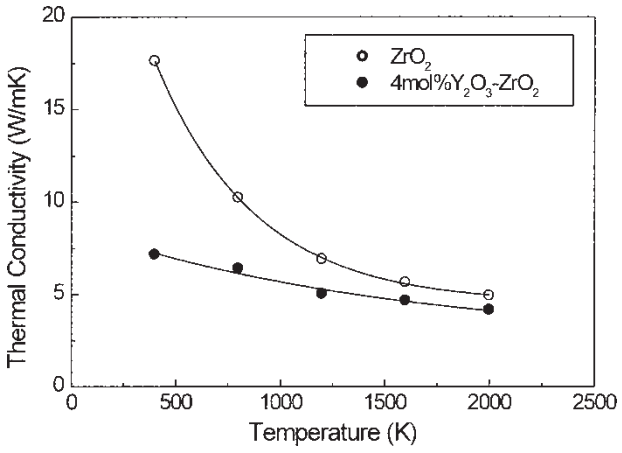

FIGURE 5 Thermal conductivity of undoped and Y_2O_3-doped ZrO_2 as a function of temperature. Data were obtained by averaging instantaneous thermal conductivities for 300 ps.

addition observed experimentally was also reproduced well. A smaller temperature dependence was observed in the case of Y_2O_3-doped ZrO_2, which can be explained in terms of phonon scattering, assuming Matthiessen's rule [1], using the phonon mean free path relation [38].

$$\frac{1}{\lambda} = \frac{1}{\lambda_i} + \frac{1}{\lambda_d} \tag{28}$$

where λ_i and λ_d are phonon mean free paths due to phonon–phonon scattering and scattering by defects, respectively. λ is the mean free path of the system which is related to the thermal conductivity of the system by Refs. [1,29].

$$\kappa = \frac{1}{3} C v \lambda \tag{29}$$

where C and v are the heat capacity of and sound velocity in the material in question, respectively. However, the absolute value of the calculated thermal conductivity at 400 K was higher than that observed by experiment on single crystal [39]. The deviation from the experimental value can be ascribed to (a) neglect of quantum effects which overestimates the heat capacity, (b) a higher sound velocity, (c) the different crystal structure (in real materials it is monoclinic, not tetragonal), (d) absence of chemical impurities and isotopes, (e) absence of the sample edges and (f) absence of a temperature gradient as is needed in experiments. Despite the difference in the absolute values, the reproduction of the relative differences in thermal conductivities over a wide range of temperature and dopant concentrations is satisfactory, in spite of the inherent limitations of the classical molecular simulation technique and simple Buckingham-type interatomic potentials. Overall, the results indicate that thermal conductivity analysis by the perturbation method is an effective tool for analyzing heat conduction mechanisms in ionic crystals.

CONCLUSION

The MD perturbation method was modified to calculate the thermal conductivity of ZrO_2 and Y_2O_3-doped ZrO_2. The energy flux vector and perturbation tensor were formulated so as to include only phase space variables in addition to a convergence parameter. The characteristics of the perturbation method were examined using ZrO_2 as a model ionic crystal. The energy flux due to the perturbation, which is equivalent to that used in Green–Kubo integration, exhibited long time-scale oscillations due to the long-range nature of Coulombic interaction. It converged at around 150 ps after the perturbation was applied. In the linear response regime, thermal conductivity was independent of the only arbitrary parameter, F_{ext}, but F_{ext} plays an important role in diminishing thermal noise in the energy flux. An exponential relationship between thermal conductivity and maximum F_{ext} that allows the system to stay within the linear response regime was found. This enables a suitable F_{ext} to be estimated prior to the simulation for a range of ionic solids. The temperature dependence of the thermal conductivity of undoped ZrO_2 and Y_2O_3-doped ZrO_2 calculated using this method reproduced experimental results well.

Acknowledgements

The authors wish to thank Prof. N. Ohtori and Dr K. Takase at Niigata University, Japan, and Dr B. Bernu at Université Pierre et Marie Curie and CNRS, France, for valuable discussions on heat flux in Coulombic system. Critical reading of the manuscript and useful suggestions by Dr C.A.J. Fisher (JFCC) are also gratefully acknowledged. This work was performed as a part of the Nanostructure Coating Project carried out by the New Energy and Industrial Technology Development Organization, Japan.

References

[1] Ziman, J.M. (1960) *Electrons and Phonons* (Oxford University Press, Oxford, UK), Chapter 8.
[2] Klemens, P.G. (1969) "Theory of thermal conductivity in solids", In: Tye, R.P., ed, *Thermal Conductivity* (Academic Press, London), Vol. 1, pp 1–68.
[3] Ashurst, W.T. and Hoover, W.G. (1972) "Non-equilibrium molecular dynamics: shear viscosity and thermal conductivity", *Bull. Am. Phys. Soc.* **17**, 1196.
[4] Bresme, F., Hafskjord, B. and Wold, I. (1996) "Nonequilibrium molecular dynamics study of heat conduction in ionic systems", *J. Phys. Chem.* **100**, 1879.
[5] Schelling, P.K. and Phillpot, S.R. (2001) "Mechanism of thermal transport in zirconia and yttria-stabilized zirconia by molecular-dynamics simulation", *J. Am. Ceram. Soc.* **84**, 2997.
[6] Schelling, P.K., Phillpot, S.R. and Keblinski, P. (2002) "Phonon scattering at a semiconductor interface by molecular-dynamics simulation", *Appl. Phys. Lett.* **80**, 2484.
[7] Oligschleger, C. (1999) "Simulation of thermal conductivity and heat transport in solids", *Phys. Rev. B* **59**, 4125.
[8] Ladd, A.J.C., Moran, B. and Hoover, W.G. (1986) "Lattice thermal conductivity: a comparison of molecular dynamics and anharmonic lattice dynamics", *Phys. Rev. B* **34**, 5058.
[9] Bernu, B. and Hansen, J.P. (1982) "Thermal conductivity of a strongly coupled hydrogen plasma", *Phys. Rev. Lett.* **48**, 1375.
[10] Lindan, P.J.D. and Gillan, M.J. (1991) "A molecular dynamics study of the thermal conductivity of CaF_2 and UO_2", *J. Phys.: Condens. Matter* **3**, 3929.
[11] Takase, K. and Ohtori, N. (1999) "Thermal conductivity of molten salt by MD simulation. Optimization of calculation conditions", *Electrochemistry* **67**, 581.
[12] Takase, K., Akiyama, I. and Ohtori, N. (1999) "Thermal conductivity of silica glass at high temperature by molecular dynamics simulation", *Mater. Trans. JIM* **40**, 1258.
[13] Hirosaki, N., Ogata, S., Kocer, C., Kitagawa, H. and Nakamura, Y. (2002) "Molecular dynamics calculation of the ideal thermal conductivity of single-crystal α- and β-Si_3N_4", *Phys. Rev. B* **65**, 134110.

Downloaded At: 18:28 14 January 2011

[14] Ciccotti, G., Jacucci, G. and McDonald, I.R. (1979) "'Thought-experiments' by molecular dynamics", *J. Stat. Phys.* **21**, 1.
[15] Evans, D.J. (1982) "Homogeneous NEMD algorithm for thermal conductivity—application of non-canonical linear response theory", *Phys. Lett.* **91A**, 457.
[16] Evans, D.J. and Morriss, G.P. (1990) *Statistical Mechanics of Nonequilibrium Liquids* (Academic Press, London), pp 3–6.
[17] Gillan, M.J. and Dixon, M. (1983) "The calculation of thermal conductivities by perturbed molecular dynamics simulation", *J. Phys. C: Solid State Phys.* **16**, 869.
[18] Grover, R., Hoover, W.G. and Moran, B. (1985) "Corresponding states for thermal conductivities via nonequilibrium molecular dynamics", *J. Chem. Phys.* **83**, 1255.
[19] Motoyama, S., Ichikawa, Y., Hiwatari, Y. and Oe, A. (1999) "Thermal conductivity of uranium dioxide by nonequilibrium molecular dynamics simulation", *Phys. Rev. B* **60**, 292.
[20] Massobrio, C. and Ciccotti, G. (1984) "Lennard–Jones triple-point conductivity via weak external fields", *Phys. Rev. A* **30**, 3191.
[21] Paolini, G.V. and Ciccotti, G. (1987) "Cross thermotransport in liquid mixtures by nonequilibrium molecular dynamics", *Phys. Rev. A* **35**, 5156.
[22] Kubo, R. (1957) "Statistical-mechanics theory of irreversible processes. I. General theory and simple application to magnetic and conduction problem", *J. Phys. Soc. Jpn.* **12**, 570.
[23] Green, M.S. (1951) *J. Chem. Phys.* **19**, 1036.
[24] de Groot, S.R. and Mazur, P. (1962) *Non-equilibrium Thermodynamics* (North-Holland, Amsterdam), p 8.
[25] Gillan, M.J. (1991) "The molecular dynamics calculation of transport coefficients", *Phys. Scr.* **T39**, 362.
[26] Irving, J.H. and Kirkwood, J.G. (1950) "The statistical mechanical theory of transport processes. IV. The equation of hydrodynamics", *J. Chem. Phys.* **18**, 817.
[27] Ewald, P.P. (1921) "Die Berechnung optischer unt elektrostatischer Gitterpotentiale", *Ann. Phys. (Leipzig)* **64**, 253.
[28] Hansen, J.-P. (1986) "Molecular-dynamics simulation of Coulomb system in two and three dimensions", *Proceedings of the 97th Intl. Enrico Fermi School of Physics* (North-Holland, Amsterdam).
[29] Kittel, C. (1986) *Introduction to Solid State Physics* (Wiley, New York), pp 604–608.
[30] Bernu, B. and Vieillefosse, P. (1978) "Transport coefficients of the classical one-component plasma", *Phys. Rev. A* **18**, 2345.
[31] Yoshiya, M., Takase, K. and Ohtori, N., Private communication.
[32] Nosé, S. (1984) "A molecular dynamics method for simulations in the canonical ensemble", *Mol. Phys.* **52**, 255.
[33] Hoover, W.G. (1985) "Canonical dynamics: equilibrium phase-space distributions", *Phys. Rev. A* **31**, 1695.
[34] Parrinello, M. and Rahman, A. (1981) "Polymorphic transitions in single crystals: a new molecular dynamics method", *J. Appl. Phys.* **52**, 7182.
[35] WinMASPHYC ver. 2.0 (Fujitsu Limited, 2001).
[36] Hoover, W.G. (1986) "HOOVER: molecular dynamics", *Lecture Notes in Physics* (Springer-Verlag, Berlin), Vol. 258, pp 9–10.
[37] Hasselman, D.P.H., Johnson, L.F., Bentsen, L.D., Syed, R., Lee, H.L. and Swain, M.V. (1987) "Thermal diffusivity and conductivity of dense polycrystalline ZrO_2 ceramics: a survey", *Am. Ceram. Soc. Bull.* **66**, 799.
[38] Klemens, P.G. and Gell, M. (1998) "Thermal conductivity of thermal barrier coatings", *Mater. Sci. Eng. A* **245**, 143.
[39] Bisson, J.-F., Fournier, D., Poulain, M., Lavigne, O. and Mévrel, R. (2000) "Thermal conductivity of yttria-zirconia single crystals, determined with spatially resolved infrared thermography", *J. Am. Ceram. Soc.* **83**, 1993.

Downloaded At: 18:28 14 January 2011